

# H $\alpha$ Imaging of an Interstellar Neutral Hydrogen Shell

Paul L. Vaughan

Faculty Sponsor: Shauna Sallmen, Department of Physics

## ABSTRACT

The interstellar medium (ISM) is composed of very low-density material consisting of gas and dust. Structures form in this ISM, including interstellar shells. Exploding stars and stellar winds interacting with the surrounding ISM produce these shells. These shells are important because they play an essential role in the recycling of elements formed in stars. The shell studied in this project is relatively near the galactic plane at galactic coordinates  $(l,b) \sim (56.5^\circ, -5.5^\circ)$ . It was discovered in the neutral hydrogen SETHI dataset. High-resolution H $\alpha$  images of the ionized gas were taken at the Kitt Peak National Observatory using the WIYN 0.9-m telescope with the MOSAIC camera. Many H $\alpha$  exposures were combined into one large mosaic image to be compared to other existing images at various wavelengths. Comparing data throughout the entire spectrum allows us to investigate the interactions and processes taking place in the ISM. The data reduction processes and analysis are discussed in this paper.

## INTRODUCTION

From our frame of reference, the universe appears to be filled with stars, galaxies, and various other bright objects. The universe however is mostly just space. Although this space may appear to be empty, it is filled with a low-density gas called the interstellar medium (ISM). This is where cosmic recycling process takes place. Stars form from the material in the ISM, go through their life cycle fusing elements heavier than the original hydrogen and helium, and later die replenishing the ISM with heavier materials for the next generation of star formation. When stars are massive enough, they explode in brilliant supernovae, disturbing the ISM. Disturbances from supernovae as well as strong stellar winds at various stages of stellar evolution push material into the ISM causing irregularities. Often the irregularities are shell-shaped, as material propagates outward from the central star. As the shell expands, it slows as it interacts with the surrounding ISM. The gas eventually cools, allowing electron recombination producing H $\alpha$  emission. Once the shell has cooled enough, the neutral hydrogen (HI) shell will be detectable through the 21-cm (radio) emission line. Since the areas of disturbance in the ISM are where the next generation of stars is formed, a strong knowledge of the properties of the ISM is needed to understand stellar and galactic evolution.

The physical state and evolution of the gasses in the ISM have been explained by different models, but it is not yet clear which theory and/or theories are correct. The McKee and Ostriker (1977) theory is a three-phase model in which the gas goes through a cold, warm, and hot phase. In the Galactic fountain model of Shapiro and Field (1976), the hot gas is pushed out of the galactic plane, the gas cools, and then the gas falls back into the Galactic plane. The third theory by Cox and Smith (1974), and Slavin and Cox (1993), states that there are more focused effects of supernovae rather than ambient material. These and other theories still have many problems that do not properly model the ISM. Studying supernova remnants and their interactions with the surrounding ISM will improve our understanding of the processes and changes involved in the ISM. Observing supernova remnants at multiple wavelengths and comparing the supernova remnant's properties at these wavelengths, which is synonymous with observing gas at various temperatures, will give a better understanding of the heating and cooling in the ISM. The Cygnus Loop Supernova Remnant is an example of this method. This supernova remnant was studied at radio, optical, far-ultraviolet, and x-ray wavelengths giving researchers both spectroscopic and image data for analysis (Heiles, Haffner, & Reynolds 1999). Combining information from the various wavelengths has given astronomers a more detailed understanding of this astronomical object.

Undergraduate research student Kurt Grunwald and faculty sponsor Dr. Shauna Sallmen identified the shell studied in this project in the Search for Extraterrestrial HI (SETHI) database. This database is a compilation of velocity-resolved cold, neutral hydrogen maps taken with the Arecibo radio telescope at wavelengths near 21cm (Korpela et al. 2002). The SETHI radio survey had better resolution and sensitivity than any preceding survey

yielding identification of shells previously overlooked. Observing these shells will give a larger survey of the interactions in the ISM and allow us to obtain better knowledge of the processes involved. Figure 1 shows the shell for this project identified in the SETHI radio image.

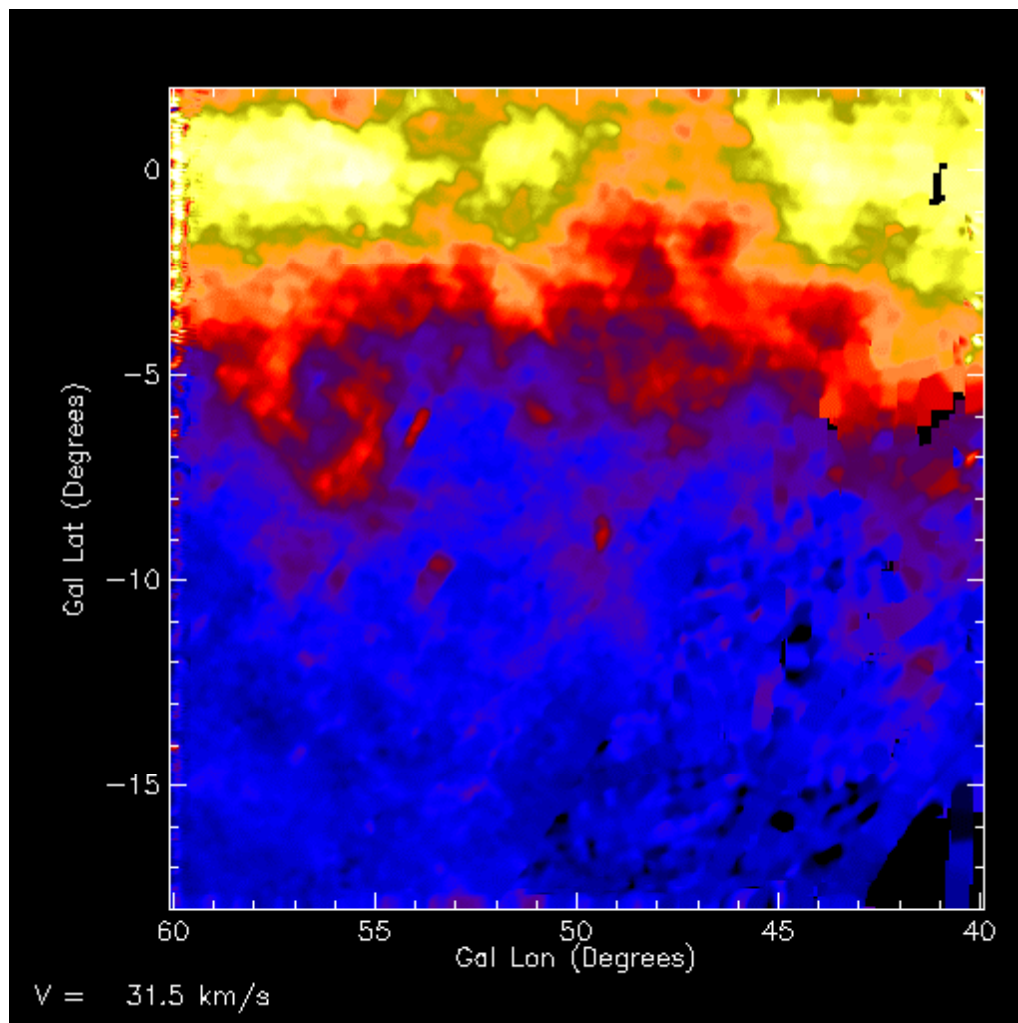


**Figure 1.** This is the SETHI image of the shell, showing neutral Hydrogen.

This shell, located at  $(l,b) \sim (56.5^\circ, -5.5^\circ)$ , is approximately five degrees by five degrees across the night sky. The project maps the shell at high angular resolution at the  $H\alpha$  wavelength of 656.281nm. Emission at this wavelength originates from the warm hydrogen of this shell and ionized electrons recombining with the hydrogen nucleus emitting energy in the  $H\alpha$  emission line. This  $H\alpha$  map will be used to compare with the other maps at various wavelengths for this shell. Comparing the different wavelengths will give astronomers a greater knowledge of the differing ways the various temperatures of gas interact with each other in the ISM.

## OBSERVATIONS

The images for this project were taken using the 0.9m WIYN telescope at the Kitt Peak National Observatory near Tucson, Arizona. The data were acquired with the use of the MOSAIC camera, composed of 8 CCD chips that form an 8k x 8k pixel array that can image nearly one square degree of the sky. One quarter of this shell was observed on June 3-7, 2006. The shell's images were taken with 20-minute exposure times using the  $H\alpha$  k1009 filter that has a central wavelength of 657.474nm and a full-width half-max of 8.062nm. Sixty-second exposures were taken of the same region with an R filter to allow continuum removal during the data reduction process. As can be seen in the planned mapping of the shell (Figure 4), images were taken in staggered sets of three with an offset of 450 arcseconds in right ascension and 250 arcseconds in declination between each image to fill the gaps between the

CCD chips. Other images, such as flats and zeros, used during the data reduction procedures, were also acquired for later correction of the raw images.

## DATA REDUCTION AND ANALYSIS

A sample raw image is displayed in Figure 2. For later reference, chip numbers are labeled in the left corners of each chip in Figure 2. The data were reduced using IRAF (Image Reduction and Analysis Facility; Tody 1986 and 1993), a data reduction package that runs under Linux. IRAF performs many corrections for instrumental effects in the data. The IRAF package was also used to combine all of the separate data into one mosaic image.

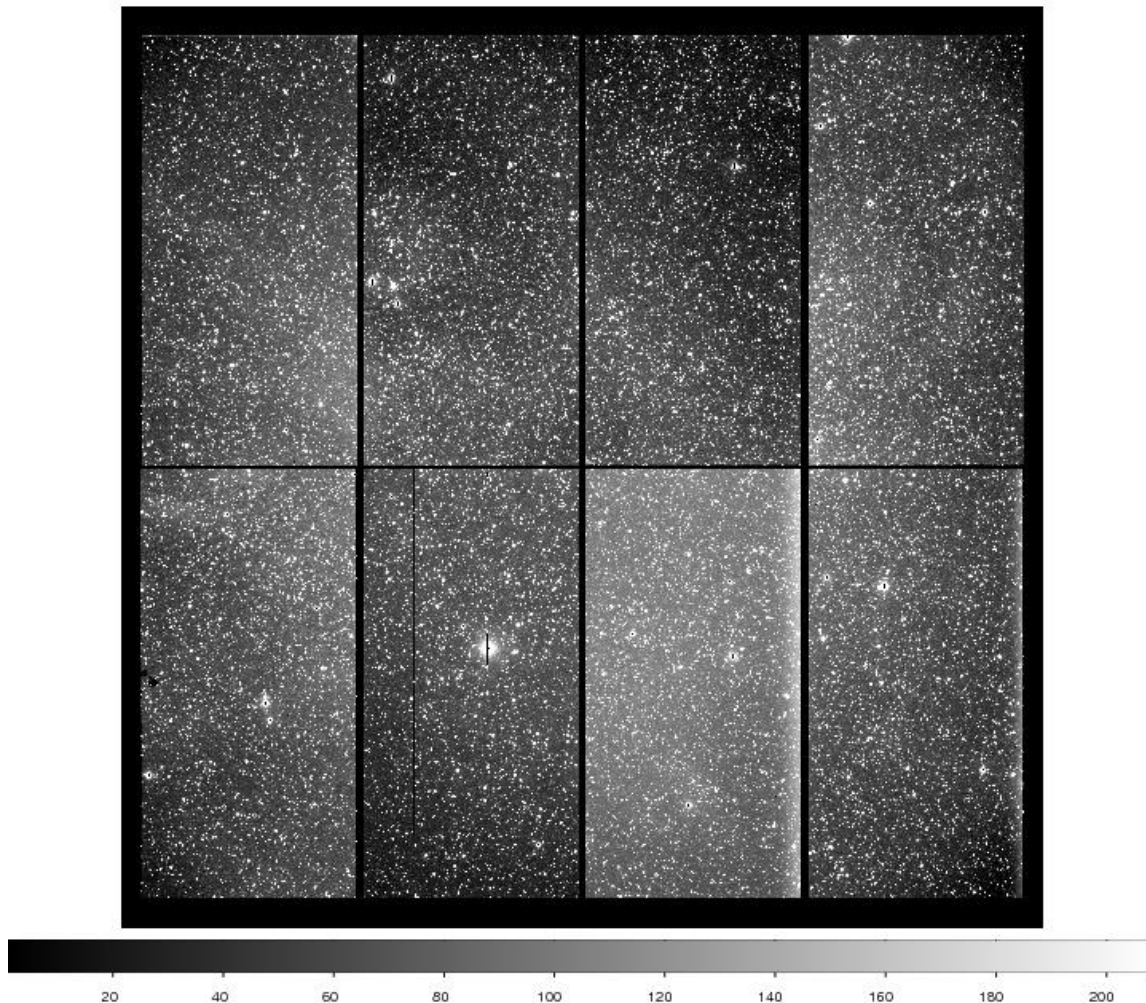


**Figure 2.** An image of raw data from this project.

The first few steps in the data reduction process corrected for the way the data were taken and stored at the telescope. Two processes, *ccdedit* and *imreplace*, were used to set a saturation value of 65000 ADU (analog-to-digital units). These tasks took negative pixel values (black center of bright star as seen in Figure 2, chip 2, near the center of the chip) caused by rollover in the analog to digital conversion process, and assigned them a value larger than the saturation level of 65535 ADU. These and other saturated pixels were later flagged in a bad-pixel mask so they could be corrected during the stacking process.

Next, we combined our zero (bias) images and our twilight sky flat images into master zeros and master flats. These were later applied to the object images to correct for instrumental effects. The zero or bias correction is necessary to account for read-out noise from the CCD chip. This read-out noise changes spatially across the CCD chip, and varies over time due to the temperature variation of the CCD. The noise is seen in Figure 2 and Figure 3a as a bright vertical band on the right side of chip 3. The zero files accounts for the variations in zero-level from chip to chip as well, seen as variations in brightness between chip 3 and the surrounding chips in Figure 2 and Figure 3b.

There is also an over-scan region in each chip (not shown) that measures the variation of the bias level throughout time. The task *zerocombine* calls *ccdproc*, which corrects for the crosstalk (large signal from one circuit transfers onto another nearby circuit), uses the over-scan region to remove temporal variations (zero will then only contain spatial variations), and trims out the edges of the chips. Then the task combines the zero images into a master zero file. This master zero (see Figure 3a) was later used to correct the science images for the effects of bias.

Next, the master flat was created to correct for pixel-to-pixel variations. These occur from differing sensitivities to light throughout the CCD causing brightness variations across the image. These can be seen in Figure 2 and Figure 3b, particularly on chip 6 (the change from light to dark and back to light). Flat fielding also corrects for dust doughnuts (circles that look like little doughnuts) as seen in Figure 3b, chip 5, at the middle of the right edge. The effects on the science images are more obvious at a larger magnification. The flats that this project used were twilight sky flats. Since the sky flats contained stars, the stars had to be removed before the flats were applied to the science images. To do this, we used *crmedian* to apply a median filter and create a clean flat with no stars. The images were processed for crosstalk, over-scan, and trim corrections with *flatcombine*, which also applied the bias correction using the master zero, and then combined the images into a master flat to be used to process the science images.

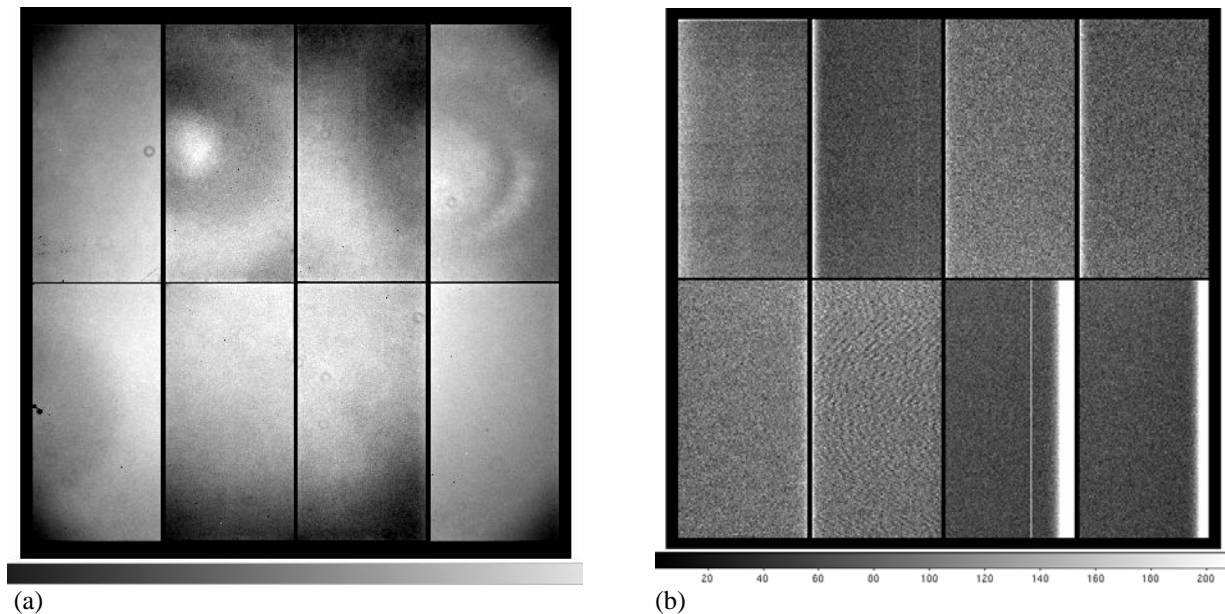


**Figure 3.** Left Panel (a) is a master zero file, and right panel (b) is a master flat file

The main processing was accomplished with *ccdproc*. *Ccdproc* provides the same corrections to the science images such as crosstalk, over-scan, and trim; however, it also applies a bad pixel mask used later in the stacking procedures and applies the zero and flat field corrections using the master zero and master flat.

As noted earlier, the science images of this shell were taken in sets of three, offset slightly, as seen in Figure 4. The shaded region of Figure 4 corresponds to current data on the shell. Each science image was aligned and stacked with overlapping images to create a single large map of this region of the shell. By stacking the images, not only were the gaps between the CCDs removed, but also the bad pixels were removed from the final image. To align the images for stacking, a world coordinate system (WCS) comprised of a catalog of stellar coordinates by magnitude was utilized. Aligning these images to the WCS using many stars on each chip corrected for the non-linear spatial scale of the CCD and allowed an unambiguous overlaying of images.

Before the images were stacked the eight CCD chips were combined into one using the task *mscimage*. This allowed the stacking task, *mscstack*, to view each pointing as one image and compute the proper overlaying of the other pointings. The product of the overlaid shells is shown in Figure 5 and is correlated to the shaded gray area in Figure 4.

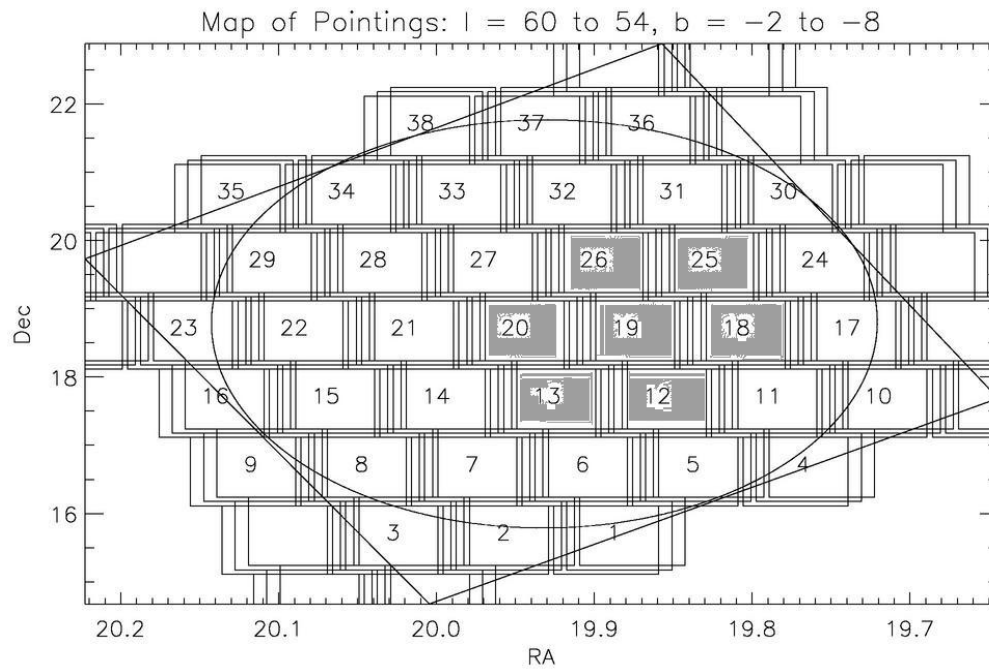


**Figure 4.** The scheduled mapping of the shell. Shaded regions corresponds to existing data.

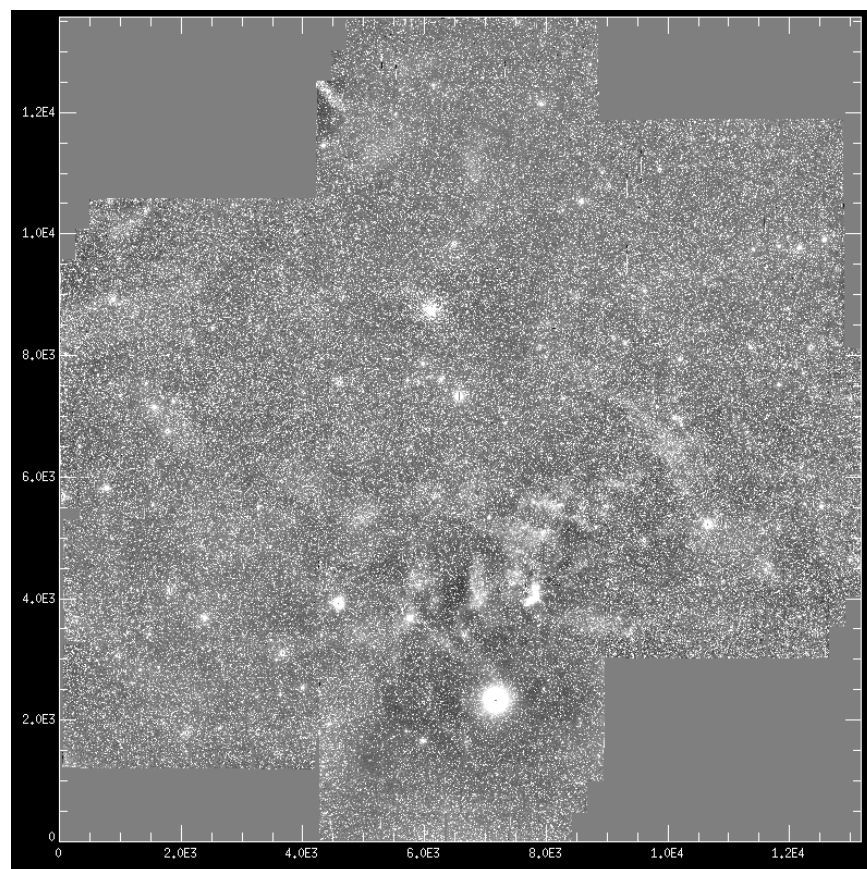


**Figure 5.** The stacked and processed science images.

The last step in processing data is to remove the stars. Although in some areas of the science images you are able to see  $H\alpha$  gas, the stars overpower the faint diffuse gas. When the stars are removed from the stacked images, a mosaic of ionized hydrogen gas is created for our specific shell. We are able to use this mosaic for comparison of other images of different gas temperatures to learn more about the evolution and processes of this interstellar shell. A trial median filter was used in Figure 6 which removed most of the fainter stars, and allows us to see more of the ionized hydrogen gas.

## CONCLUSION

The white box in Figure 7 encloses the neutral-hydrogen map of the shell in the region corresponding to Figure 6. As seen in the comparison of these two images, a large amount of hot ionized hydrogen gas is correlated with a gap in the neutral hydrogen wall of the shell. The gas in this region is warmer and has not yet cooled enough to be neutral. The shell has not been completely observed however, so we are unable to see if this characteristic is ubiquitous throughout the entire shell. Also notable in Figure 6 is an apparent bow shock, marked by a black arrow. We are currently investigating this feature to determine its origins.

Observing of the rest of this shell will be completed in the future at the Kitt Peak National Observatory. Once the new data are reduced in the same manner as described and combined with the already processed data a complete mosaic will be created. This image will be compared with existing neutral hydrogen images to enable us to study the evolution of this particular shell. Understanding this shell and comparing it to other shells will give astronomers a better understanding of the evolution and processes occurring in the interstellar medium.

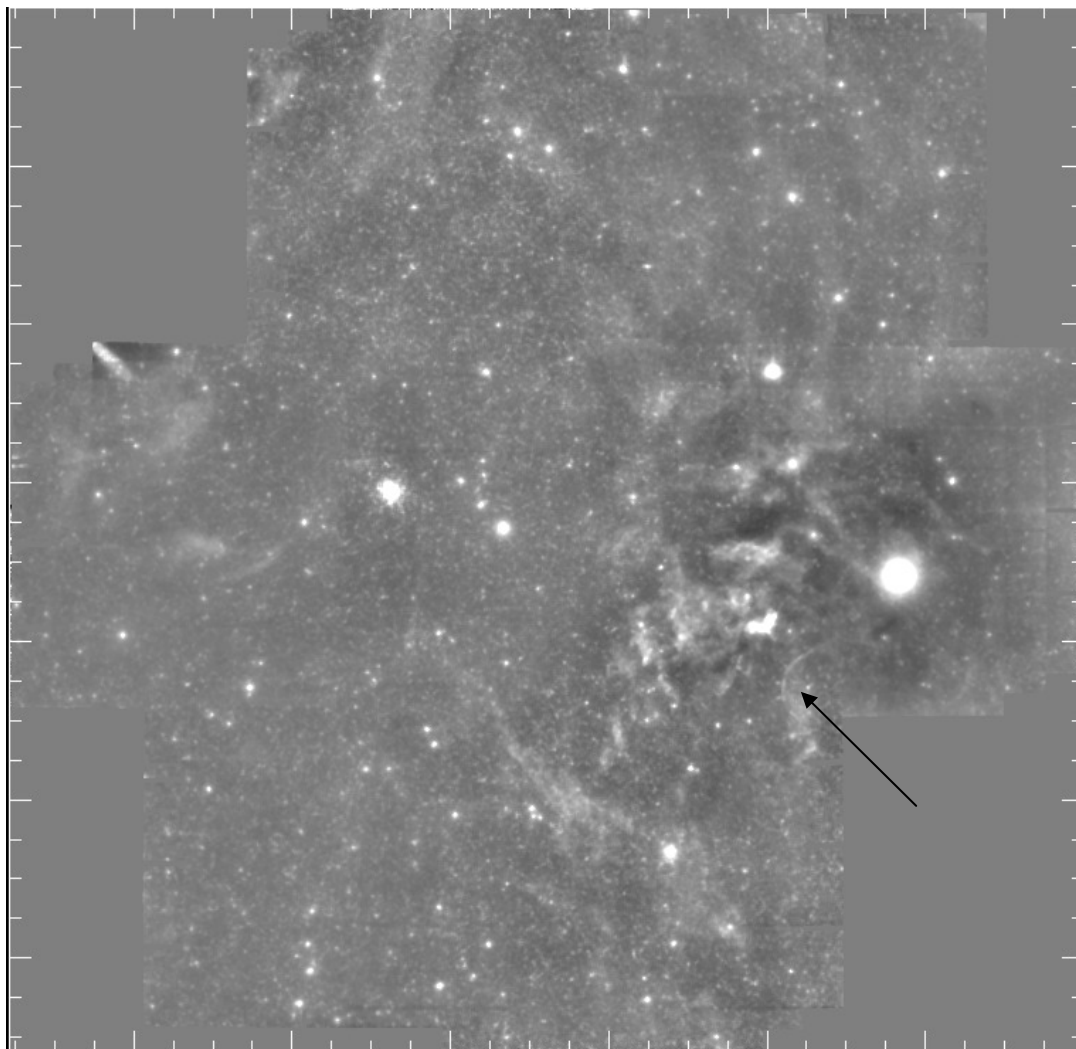


**Figure 6.** The stacked shell with a median filter to remove some stars. Arrow shows bow shock.

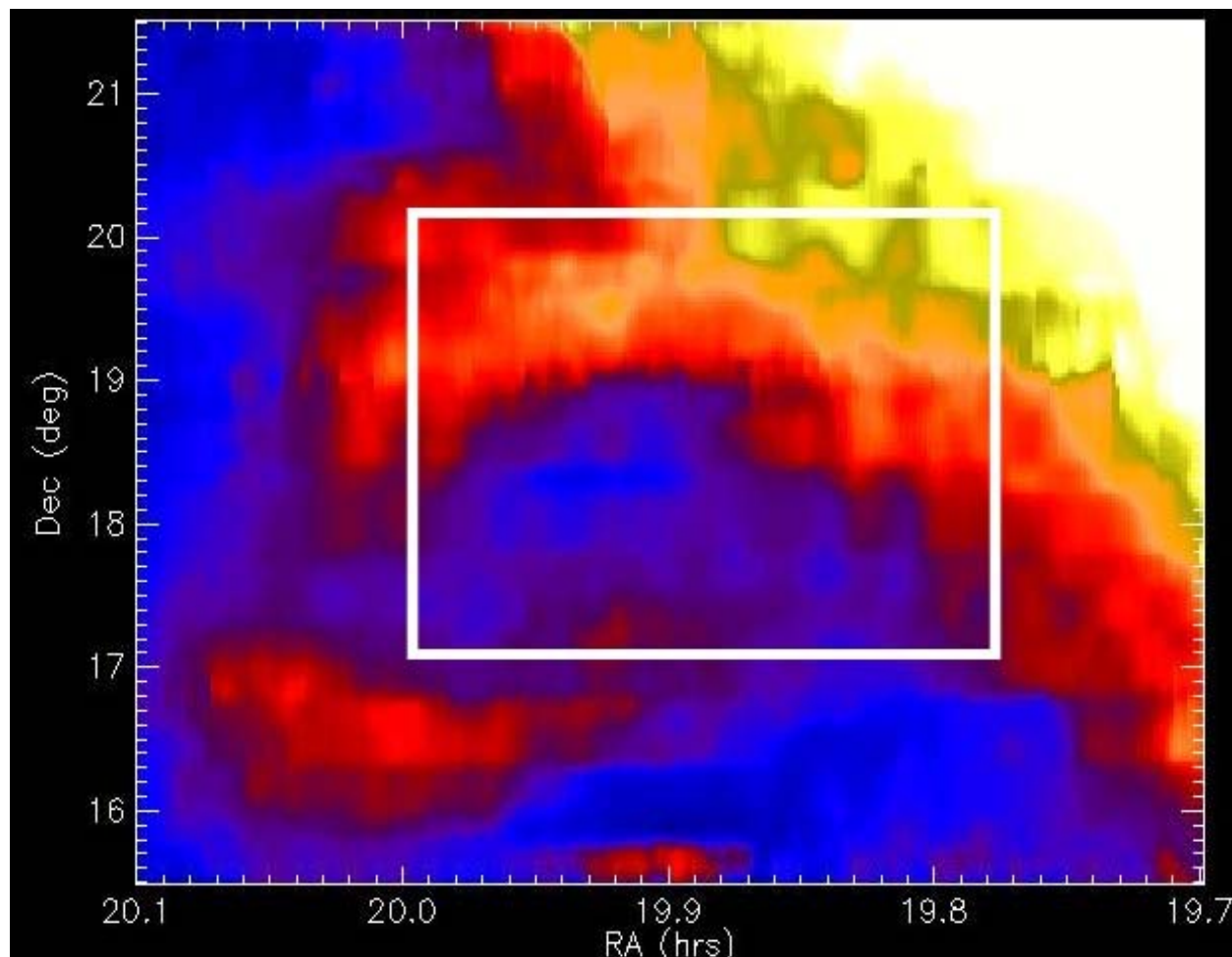


**Figure 7.** The shell mapped in neutral hydrogen in the same alignment as Figure 6. The white box is the approximate area of Figure 6.

## ACKNOWLEDGEMENTS

This research was supported by the National Science Foundation, Research Corporation, Wisconsin Space Grant Consortium, and the UW-L SAH Dean's Distinguished Fellowship.

## REFERENCES

- Cox, D. and Smith, B. (1974), 'Large scale effects of SNRs on the Galaxy: Generation and Maintenance of a Hot Network of Tunnels', *The Astrophysical Journal*, 189, L105
- Heiles, C., Haffner, L.M. & Reynolds, R.J. (1999), 'The Eridanus Superbubble in its Multiwavelength Glory', in ASP Conf. Series 168, p211, Ed. A.R. Taylor, T.L.Landecker & G. Joncas (San Francisco: ASP)
- Korpela, E. et al (2002), 'SETHI@Berkeley - A Piggyback 21-cm Sky Survey at Arecibo' in ASP Conf. Series 276, p100, Ed. A.R. Taylor, T.L. Landecker & A. Willis (San Francisco: ASP)
- McKee, C. and Ostriker, J. (1977), 'A theory of the interstellar medium', *The Astrophysical Journal*, 218, 148
- Shapiro, P. & Field, G. (1976), 'Consequences of new hot component of the ISM', *Astrophysical Journal*, 205, 762
- Slavin, J. & Cox, D.P. (1993), 'Evolution of SNRs in a Warm Diffuse Medium', *Astrophysical Journal*, 417, 187
- Tody, D. (1986), "The IRAF Data Reduction and Analysis System" in Proc. SPIE Instrumentation in Astronomy VI, ed. D.L. Crawford, 627, 733
- Tody, D. (1993), "IRAF in the Nineties" in *Astronomical Data Analysis Software and Systems II*, A.S.P. Conference Ser., Vol 52, eds. R.J. Hanisch, R.J.V. Brissenden, & J. Barnes, 173.